The RNase H affinity and cleavage of the target RNA in the antisense–RNA hybrid duplexes containing various 3′-tethered substituents in the antisense strand

Nariman V. Amirkhanov and Jyoti Chattopadhyaya *

Department of Bioorganic Chemistry, Box 581, University of Uppsala, Biomedical Center, S-75123 Uppsala, Sweden. E-mail: jyoti@bioorgchem.uu.se; Fax: +4618-554495; Tel: +4618-4714577

Received (in Cambridge, UK) 10th September 2001, Accepted 6th November 2001
First published as an Advance Article on the web 17th December 2001

The kinetics of RNase H promoted cleavage of the RNA strand in the antisense oligonucleotide (AON)–RNA hybrid duplexes, with the 3′-end of the AON strand tethered with cholic acid (**2**), its triacetate (**3**), cholesterol (**4**) or dipyridophenazine (**5**), have been investigated by changing the concentration of both the AON and the RNA strands, while keeping the enzyme and the buffer concentration constant. It has been shown that the extent of the cleavage of the target RNA by RNase H in the conjugated AON (**2**–**5**)–RNA (**6**) hybrid duplexes, at saturation conditions for RNA in the presence of an excess of AON, is higher than in the native 9mer AON (**1**)–RNA (**6**) duplex. The RNA concentration-dependent kinetics of the RNase H promoted cleavage reaction gave values for K_m and V_{max} for RNA (**6**)–AON (**1**–**5**) duplexes. The V_{max} values for all 3′-tethered AON–RNA duplexes were ~30% less efficient, and their K_m were also 4–14 times less, than the native counterpart, which means that the 3′-tethered substituent decreases the catalytic activity of RNase H owing to the increased affinity toward the enzyme. Since the values of V_{max} and K_m change in a compensating manner at a fixed enzyme concentration, the V_{max} : K_m ratio for all 3′-tethered AONs in the corresponding AON–RNA duplexes showed the unique nature of the 3′-tethered substituent, dictating the 3′-substituent-dependent enzyme affinity of the heteroduplex, in comparison with the native. Accordingly, 3′-tethered Dppz AON (**5**)–RNA duplex has a maximum affinity for RNase H, ~6-fold more compared to the native 9mer (**1**), and ~2-fold more compared to 3′-tethered cholic acid (**2**), its triacetate (**3**) or cholesterol (**4**) containing AON–RNA duplexes.

Introduction

RNase H occurs widely in various organisms, both in eukaryotes and prokaryotes.[1–7] Various isotypes of RNase H seem to have similar nucleolytic activity and substrate requirements.[7–12] It has very limited sequence specificity, and requires Mg^{2+} ions to cleave the target RNA in DNA–RNA hybrid duplexes in an endonucleolytic manner between 3′–O and 5′–P in the internucleotidyl 3′–**O–P**–O–5′ bond to produce 5′-phosphate and 3′-hydroxy ends[7,13] (Scheme 1). Several affinity studies have been so far performed to understand the substrate tolerance, specificity and preferences for modifications in the DNA (*i.e.* the antisense) strand of the hybrid duplex[8–12] (Scheme 1). It has emerged that the RNA in the various 2′-*O*-modified chimeric antisense oligonucleotide (AON) substrates (*e.g.* F, OMe, OPr, OCH_2–OEt *etc.*) was digested by RNase H *ca.* 3-fold more slowly than the wild type duplexes.[9a] It has been recently shown from various laboratories that incorporation of 3′-*endo* conformation constrained[9] nucleotide preorganizes (both because of the combined forces of stereoelectronic gauche and anomeric effects[14,15]) the antisense strand into an A-RNA type conformation, inducing the heteroduplex conformation into an RNA–RNA type duplex. This conformational mimicry by the AON–RNA heteroduplex enhances its stability,[16a–j] but that, more often than not, results in a reduced catalytic RNase H promoted cleavage of the RNA strand in the heteroduplex.[12,16] We have however found one exception to this with our oxetane system: [1-(1′,3′-*O*-anhydro-β-D-psicofuranosyl)thymine].[17a–c] The introduction of the north-east constrained oxetane system ($20° < P < 45°$, $27° < \varphi_m < 35°$)[15] in the antisense strand reduces the heteroduplex stabilities (~6 °C per modification).[17a,b] The introduction of up to 3 oxetane modifications in the AON strand (*i.e.* reduction of T_m by ~18 °C) were nicely tolerated by RNase H, without any concomitant reduction of the rate of the RNase H cleavage reaction of the complementary RNA,

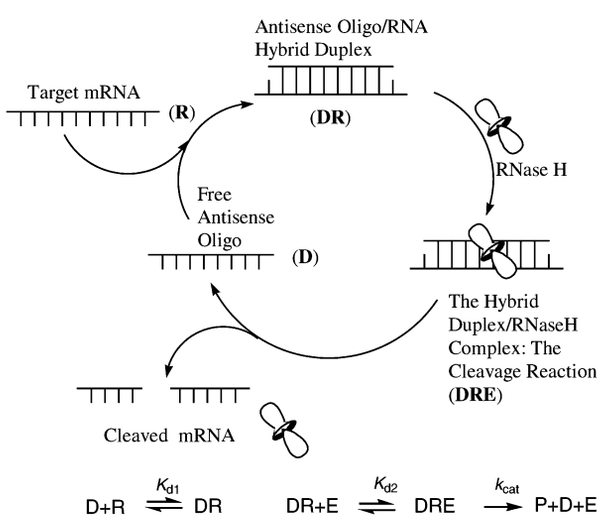

Scheme 1 The catalytic RNase H promoted cleavage of the target mRNA through the formation of an antisense oligo–RNA hybrid duplex. The kinetic scheme for the RNase H hydrolysis is shown in the bottom part of the cartoon, where **D** is AON; **R** is the target RNA; K_{d1} is the equilibrium constant of dissociation of the heteroduplex **DR**; K_{d2} is the equilibrium constant of dissociation of the substrate–enzyme complex **DRE**.

DOI: 10.1039/b108196a

compared to the wild type heteroduplex.[17c] We are obviously intrigued by this new finding, in view of what is known about RNase recruitment *vis-à-vis* conformational preorganization in the AON–RNA heteroduplexes by the AON.[7,9,10]

In order to understand some of the underlying factors controlling the heteroduplex stability *vis-à-vis* catalytic RNA cleavage by RNase H in the AON–RNA heteroduplex[18a–e] (Scheme 1), we here report the results of our kinetic studies on the RNase H binding affinity of AON–RNA heteroduplexes, as well as the catalytic cleavage rate of the complementary RNA strand in these heteroduplexes, containing AONs with the 3′-tethered aromatic or alicyclic substituents such as dipyridophenazine (Dppz), cholic acid (Chol), cholic acid triacetate (Chol-$(Ac)_3$) and cholesterol (Cholest).

Results

The stabilities of the heteroduplexes containing AONs tethered to different aromatic groups and the complementary RNA increases because of the stacking interaction of the tethered ligand with the AON–RNA helix, without compromising the RNase H promoted cleavage rate of the complementary RNA strand by RNase H.[18a–e] It was found that amongst all 3′-aromatic tethered AONs, the introduction of the 3′-Dppz moiety enhances the extent of RNase H cleavage of the target RNA in the RNA–AON hybrid duplexes most in comparison with the native 9mer AON.[18d,e] To our surprise, phenazine (Pzn) and positively charged phenazinium ($Pznm^+$) groups at the 3′-end of the conjugated AON in the AON–RNA hybrid have very similar effects on the RNase H promoted cleavage activity compared with the native 9mer AON, suggesting that RNase H does not have the ability to discriminate between a neutral and the positively charged chromophore.[18d] Earlier, it was also established by detailed NMR spectroscopy that the reason for duplex stabilization by 3′-tethered aromatic groups, such as phenazinium ($Pznm^+$),[19a] is owing to its stacking interaction with the neighboring nucleobases, which reduces the level of hydration in the minor and major grooves, compared to the native, thereby stabilizing the hydrogen bonds.[19b–d]

We here report on the influence of the biologically important 3′-hydrophobic groups tethered AONs (**2**–**4**) such as cholic acid[20a–e] in **2**, 3,7,12-tri-*O*-acetylcholic acid[20b,e] in **3** and cholesterol[20f,g] in **4** on the extent of complementary RNA cleavage in the AON–RNA duplexes by RNase H, and compared them with 3′-tethered Dppz[21] in **5**, and the native AON counterpart[22a] (**1**) (Scheme 2).[20a,b,f,21,22] These hydrophobic groups were chosen because of the following reasons: (i) they have been shown to increase penetration of AONs inside the cells,[23a–d,20d–g] (ii) the AONs with these groups also show an increase in the resistance against 3′-exonucleases,[18d,23a,c,d] (iii) these groups might assist in the liver-specific drug-targeting and/or hepatocellular uptake,[20d] and (iv) these bile acids are also involved in the digestion and resorption of fats in the small intestine, and the majority of bile acids is reabsorbed and transported with portal blood back to the liver (enterohepatic circulation), which is repeated up to 15 times per day. Thus this high transport capacity could be taken advantage of by conjugating antisense oligos with the bile acids.[20c]

Thermodynamic stabilities of all AON(**1**–**5**)–RNA (**6**) hybrid duplexes are shown in Scheme 2. It was found that all 3′-tethered AONs (**2**–**5**)–RNA (**6**) duplexes are more stable (ΔT_m ranges from +4 to +11 °C) compared to the native 9mer AON (**1**), and that the 3′-Dppz group makes the corresponding AON (**5**)–RNA (**6**) duplex more stable ($\Delta T_m = +11$ °C) than the other 3′-tethered AONs **2**–**4**.

The extent of RNA cleavage by RNase H in all AON (**1**–**5**)–RNA (**6**) duplexes was investigated both (i) by changing the AON concentration (Figs. 1–3) at constant concentration of RNA and RNase H in order to obtain saturation conditions for RNA (*i.e.* when RNA is completely bound to the AON in the duplex form) in the presence of an excess of AON, and also (ii) by changing the RNA concentration (Figs. 4–6) at a constant concentration of RNase H and AON, which is sufficient for complete saturation of RNA. The initial velocities (v_0) have thus been obtained at four different RNA concentrations (ranging from 0.123 μM to 2.02 μM) (Fig. 5 and Table 1) at saturating conditions for RNA (**6**) by AON (**1**–**5**) (10 μM), which were subsequently plotted as a function of substrate, RNA–AON hybrid duplex, concentration (S_0) to give K_m and V_{max} from both the Michaelis equation and Lineweaver–Burk analysis.[24]

The summary of our investigation is as follows.

The extent of the target RNA cleavage by RNase H in the hybrid RNA (**6**)–AON (**2**–**5**) duplexes at saturation conditions (when RNA is completely saturated by AON at low RNA concentration) is higher than in the native 9mer AON (**1**)–RNA (**6**) duplex (Figs. 1–3).

When the AON concentration for **1**–**5** is increased, we see an increase in the extent of cleavage along with the increase in the height of the saturation plateau (Fig. 3). The plot of this AON concentration-dependent study is hyperbolic in nature, which appears sigmoidal in shape in the logarithmic scale [AON] plot as shown in Fig. 3. This is contrary to what was reported[20g] earlier for cholesterol tethered AON (**4**), where it was shown to have a parabolic dependence of the extent of cleavage with increasing AON concentration, or to show a decrease of the RNase H response at a high concentration of AONs.[20g]

For AONs containing cholic acid (**2**), cholic acid triacetate (**3**) and cholesterol (**4**), the cleavage sites have been found to be both at U9 and G12 positions in *ca.* 1 : 4 ratio (Fig. 1) of the complementary target RNA compared to that of the native 9mer AON (**1**), which had only a single cleavage site at the G12 position (Fig. 1). This shows that at least there are two binding sites as well as the cleavage sites in AONs (**2**–**4**)–RNA compared to that of the native counterpart.

On the other hand, the 3′-Dppz tethered AON (**5**) promotes only a single cleavage site at the U10 position of the target RNA (Fig. 1) with a maximal extent of cleavage both at the saturating and non-saturating conditions of RNA, compared to all other AONs, specially at a low AON concentration (Fig. 2A and Fig. 3), showing that the 3′-Dppz group has not only promoted higher cleavage of RNA, but also forces the RNase H to bind and cleave at distinctly different sites from those of the native as well as for AONs (**2**–**4**)–RNA duplex.

The RNA concentration-dependent kinetics of the RNase H promoted cleavage reaction (Figs. 4–6, Tables 1 and 2) gave values for V_{max} (Fig. 7A), K_m (Fig. 7B) and k_{cat} (Table 3). The estimation of K_m and V_{max} was performed by two methods: (i) from the $1/v_0$ *versus* $1/[S_0]$ plots, where $[S_0] = [RNA]$, or (ii) directly from v_0 *versus* $[S_0]$ plots,[24] which give the Michaelis dependency of v_0 from $[S_0]$ described by the equation: $v_0 = V_{max}[S_0]/(K_m + [S_0])$. Observed values of V_{max} and K_m by these methods were found to be in good agreement (Figs. 7A and 7B).

Since the $V_{max} = E_0 \times k_{cat}$ (E_0 = initial enzyme concentration), and for all of our RNA concentration dependent kinetics, the E_0 was identical, hence V_{max} is a proportional to k_{cat}. This shows that the relative k_{cat} can be understood by comparing simply the V_{max}. Fig. 7C thus shows the $V_{max}/K_m = k_{cat}/K_m$ for all 3′-tethered AONs in the corresponding AON–RNA duplexes, showing the unique 3′-tethered substituent-dependent enzyme affinity of the heteroduplex in comparison with the native counterpart. Comparison of values of V_{max}/K_m is important since V_{max} and K_m would be expected to change in a compensating manner at a fixed E_0.[8,24,25]

The V_{max}/K_m value for AON (**5**)–RNA is six-fold more than the native counterpart (Fig. 7C). On the other hand, for 3′-tethered cholic acid (**2**), its triacetate (**3**) or cholesterol (**4**) complex, the RNase binds both to the 3′-tethered ligand as well as within the heteroduplex, hence giving two different cleavage sites, which can be seen in the V_{max}/K_m value for AON (**2**–**4**)–

Table 1 Dependence of the initial velocity (v_0) on the substrate concentration [a]

[RNA] = S_0/μM	v_0/μM min^{-1}				
	9mer-AON	Chol-AON	Chol(Ac)$_3$-AON	Cholest-NAON	Dppz-AON
0.123	0.00166	0.00589	0.00487	0.00391	0.00689
0.523	0.00518	0.00786	0.00786	0.00974	0.01086
1.023	0.01180	0.01762	0.01370	0.01419	0.01604
2.023	0.01526	0.01486	0.01536	0.01386	0.01386

[a] Initial velocity has been calculated from the data taken up to 7.6 min into the reaction.

Table 2 Dependence of the extent of cleavage (P/S_0) of RNA on the substrate concentration [a]

	$\alpha = P/S_0$				
[RNA] = S_0/μM	9mer-AON	Chol-AON	Chol(Ac)$_3$-AON	Cholest-AON	Dppz-AON
0.123	0.0675	0.240	0.198	0.159	0.280
0.523	0.0495	0.0751	0.0751	0.0932	0.104
1.023	0.0577	0.0861	0.0670	0.0694	0.0784
2.023	0.0377	0.0367	0.0380	0.0342	0.0342

[a] Extent of cleavage was calculated from the data taken during the first 5 min of the reaction.

RNA, which is three-fold more than the native counterpart (Fig. 7C). Such behavior of the Dppz-AON might be associated with the structure of the Dppz moiety itself, in which two pyridyl-nitrogens (N4 and N5) in the fused phenanthroline system can form a chelated complex with divalent metal ions such as Mg^{+2}. Since Mg^{+2} ion is an important cofactor for RNase H[13,7] promoted cleavage reaction of DNA–RNA hybrid duplexes as a substrate, it is likely that the Dppz group provides important assistance by supplying Mg^{+2} ions to augment the RNase H affinity toward Dppz-AON in the corresponding hybrid duplex with RNA for subsequent RNase H cleavage.

Fig. 8 shows purities of all 3′-tethered AONs used in this work (Figs. 8A, B). It also shows (Fig. 8C) the relative retention times of a mixture of AONs **1**–**5** on a reversed-phase C18 column (solvent system: buffer A: 0.05 M $LiClO_4$, buffer B: 80% CH_3CN in 0.05 M $LiClO_4$, 0% ⟶ 100% B during 40 min, rate of elution 1.5 ml min^{-1}), showing the relative hydrophobicity of different 3′-tethered AONs, compared to the

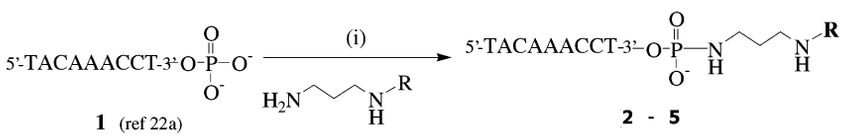

(**1**): (Native 9mer AON) $T_m = 20^oC$ ($\Delta T_m = 0^oC$)
(**2**): R = **Chol** (Chol-AON) $T_m = 25^oC$ ($\Delta T_m = 5^oC$)
(**3**): R = **Chol(Ac)$_3$** (Chol(Ac)$_3$-AON) $T_m = 24^oC$ ($\Delta T_m = 4^oC$)
(**4**): R = **Cholest** (Cholest-AON) $T_m = 25^oC$ ($\Delta T_m = 5^oC$)
(**5**): R = **Dppz** (Dppz-AON) $T_m = 31^oC$ ($\Delta T_m = 11^oC$)

(**6**): 5'-r(ACUCAUGUUUGGACUCU)-3' (Native 17mer RNA)

ΔT_m = [(T_m of (**2-5**)) - (T_m of (**1**))]

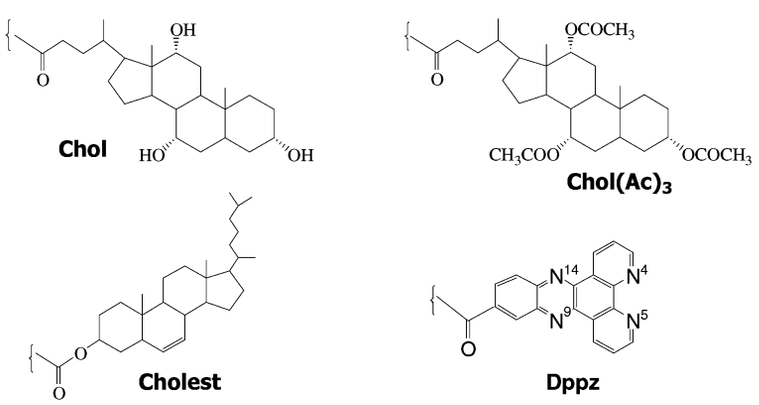

Scheme 2 Synthesis and structures of the antisense oligonucleotides, AONs, (**1**–**5**), target RNA (**6**) and the thermodynamic stability of the corresponding hybrid AON–RNA duplexes (T_m values, see Experimental section for conditions). *Reagents and conditions*. (i): 3′-phosphate-9mer (**1**) (30 OU_{260}, 0.33 μmol), triphenylphosphine (200 μmol), 2,2′-dithiodipyridine (200 μmol), 4-dimethylaminopyridine (400 μmol) and amine derivative $H_2N(CH_2)_3NHR$ (500 μmol) in dry dimethylformamide (300 μl) at RT (see ref. 22***b,c***). **Yields of 2**–**5** vary from 50–70%.

Table 3 Kinetic characteristics[a] of RNA cleavage by RNase H from AON–RNA duplex

Substrate	V_{max}/μM min^{-1}	K_m/μM	k_{cat}/min^{-1}
9mer-AON(**1**)–RNA(**6**)	$(3.19 \pm 0.45) \times 10^{-2}$	2.10 ± 0.29	16.6 ± 2.3
Chol-AON(**2**)–RNA(**6**)	$(1.93 \pm 0.71) \times 10^{-2}$	0.39 ± 0.14	10.1 ± 3.7
Chol$(Ac)_3$-AON(**3**)–RNA(**6**)	$(1.99 \pm 0.20) \times 10^{-2}$	0.58 ± 0.06	10.4 ± 1.1
Cholest-AON(**4**)–RNA(**6**)	$(1.74 \pm 0.12) \times 10^{-2}$	0.38 ± 0.03	9.06 ± 0.6
Dppz-AON(**5**)–RNA(**6**)	$(1.62 \pm 0.35) \times 10^{-2}$	0.18 ± 0.04	8.4 ± 1.8

[a] $V_{max} = k_{cat}E_0$ ($E_0 = 2 \times 10^{-2}$ U μl^{-1} = 1.92×10^{-3} μM, specific activity = 420000 U mg^{-1} = 1.134×10^{-13} moles per unit, MW = 21000 g mol^{-1}).

native, which might give us an estimate of how easily these AONs may penetrate inside the cell. It can be seen that they can be classified on the basis of their relative hydrophobicities in the following manner, as judged by their relative retention times (t_R) in the reversed-phase column: **1** (t_R = 9.9 min) < **2** (t_R = 12.6 min) < **3** (t_R = 15.4 min) < **5** (t_R = 19.9 min) < **4** (t_R = 35.6 min). We however have not found any correlation between the hydrophobicity of Chol-, Chol$(Ac)_3$- and Cholest-AONs (Fig. 8C) and theirs kinetic parameters (K_m, V_{max} and k_{cat}) (Fig. 7, Table 3). *It suggests that the recognition of AON–RNA duplex by RNase H is not associated with hydrophobic properties of the 3′-tethered moiety in the AONs, which is also consistent with the fact that 3′-tethered Pzn and Pznm$^+$ promote comparable rates of cleavage of RNA.*[18d]

Discussion

The dependence of initial velocity, v_0, of cleavage reaction from substrate concentration (S_0 = [RNA]) has been found (Fig. 5, Table 1), which can be interpreted according to the Michaelis equation [eqn. (1)]:

$$v_0 = \frac{V_{max} S_0}{K_m + S_0} \quad (1)$$

where v_0, in unsaturated conditions (when $S_0 \leq K_m$), increases with the increase of S_0, and has a saturation plateau when $S_0 \longrightarrow \infty$ (Fig. 5).

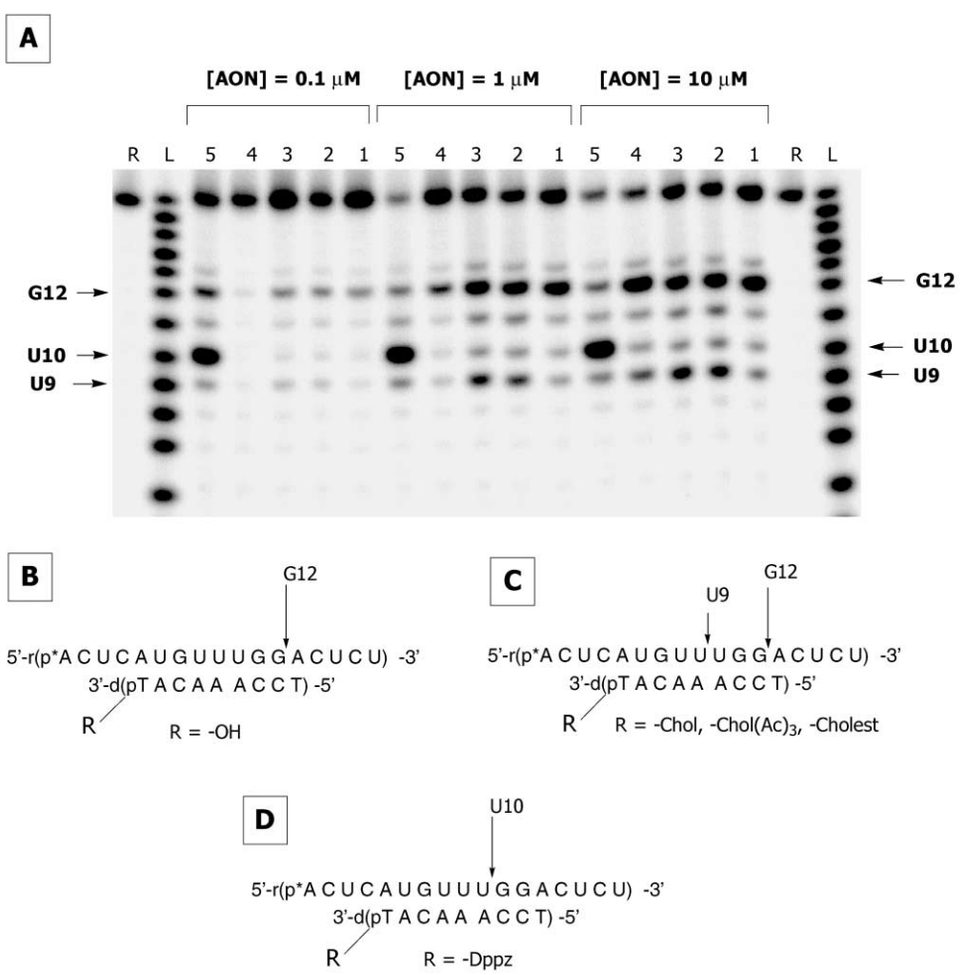

Fig. 1 (**A**) Autoradiogram of the 20% denaturing PAGE showing RNase H cleavage (after 30 min of incubation) of the 17mer target RNA (**6**) when hybridized with AONs (**1**–**5**). Lane **1**: native 9mer AON (**1**); lane 2: Chol-AON (**2**); lane 3: Chol$(Ac)_3$-AON (**3**); lane 4: Cholest-AON (**4**); lane 5: Dppz-AON (**5**); lane R: ^{32}P-labelled target RNA (**6**) without AON; lane L: snake venom PDE ladder. *Conditions of cleavage reaction*: AON (0.1 μM, 1 μM and 10 μM) and RNA (0.01 μM) in buffer, containing 20 mM Tris-HCl (pH 8.0), 100 mM KCl, 10 mM $MgCl_2$ and 1 mM dithiothreitol (DTT), 21 °C, 1 U of RNase H. Total reaction volume is 30 μl. RNase H degradation pattern of the 17mer RNA target hybridized with native 9mer AON (**B**), Chol-, Chol$(Ac)_3$- and Cholest-AONs (C), Dppz-AON (**D**). The vertical arrows with nucleotide sequence number indicate the site of cleavage on the RNA strand.

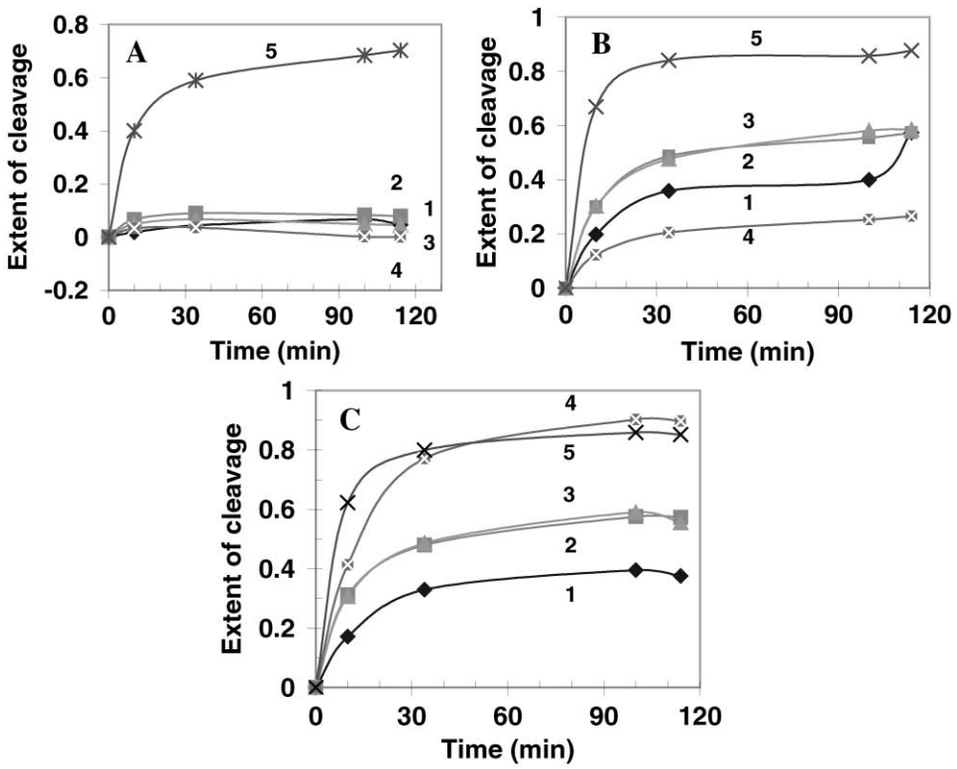

Fig. 2 The AON concentration dependent hydrolysis of the target RNA (**6**) in the AON–RNA hybrids by RNase H as a function of the reaction time. Curves 1–5 in (**A**) to (**C**) correspond to the hybrid duplexes formed by native 9mer AON (**1**), Chol-AON (**2**), Chol(Ac)$_3$-AON (**3**), Cholest-AON (**4**) and Dppz-AON (**5**), respectively, with the complementary RNA (**6**). *Conditions of the cleavage reactions*: AON concentration at 0.1 μM in (**A**), 1 μM in (**B**) and 10 μM in (**C**) with constant RNA (**6**) concentration at 0.01 μM in buffer, containing 60 mM Tris-HCl (pH 7.5), 60 mM KCl, 10 mM $MgCl_2$ and 1 mM DTT at 21 °C, 0.5 units of RNase H. Total reaction volume is 30 μl.

In this case, different AONs are working in different manners in different substrate concentration (compare the area where $S_0 < 1$ μM with the area when $S_0 > 2$ μM in Fig. 5 and Table 1). Thus, Dppz-AON (**5**) has a maximal and the 9mer AON (**1**) has a minimal cleavage reaction in the area when $S_0 < 0.2$ μM and the relative activity switches in the opposite direction in the area when $S_0 > 3$ μM (Fig. 5B).

The Michaelis equation [eqn. (1)] can be written in different forms at different substrate concentrations. (A) Under *low substrate concentrations*, when $S_0 \ll K_m$, eqn. (1) takes the form of eqn. (2).

$$v_0 = \frac{V_{max} S_0}{K_m + S_0} = \frac{V_{max}}{K_m} S_0 \qquad (2)$$

This means that v_0 is linearly dependent upon the substrate concentration with the linear coefficient of V_{max}/K_m, which is maximal for the duplex formed with Dppz-AON (**5**) and minimal for the duplex formed with 9mer AON (**1**) (Fig. 7C). (B) Under *large substrate concentrations*, when $S_0 \gg K_m$, eqn. (1) can be rewritten as eqn. (3).

$$v_0 = \frac{V_{max} S_0}{K_m + S_0} = V_{max} = k_{cat} E_0 \qquad (3)$$

This means that the initial velocity of the reaction in this case is dependent only on V_{max} or, alternatively, on k_{cat} and E_0. The initial velocity or efficiency of the reaction in this case is dependent on V_{max}, which for all 3′-tethered AON–RNA duplexes is ~30% less efficient than the natural counterpart, which means that the 3′-tethered substituent decreases the catalytic activity of RNase H. The V_{max} is maximal for native 9mer AON and relatively less for Dppz-AON (Fig. 7A and Table 3).

It is known that RNase H concentration under the physiological conditions is *ca.* 10^{-3}–10^{-2} micromoles per litre[7a] and mRNA concentration is *ca.* 10^{-2}–10^{-1} micromoles per litre.[7a] It means that our conjugated AONs are working (Fig. 5) with improved efficiency under putative physiological conditions compared with the native 9mer AON, when [RNA] = 0.1 micromoles per litre. Under a constant RNase H concentration and time, but with a large substrate concentration and rich saturation conditions for the enzyme, v_0 should be maximal for the native 9mer AON, but the extent of cleavage, since that is not dictated by K_m or $[S_0]$, will be low for all AONs because the amount of product formation will be the same. Clearly, the extent of the RNA cleavage, α, will be low if the initial substrate concentration $[S_0]$ is high, and in this case, it is possible to cleave only a small part of the initial mRNA. So, v_0 of the reaction does not say very much about the extent of final cleavage, $\alpha = [\Delta P]/S_0$, where $[\Delta P]$ is product of cleavage in the reaction time Δt.

For this reason we have investigated also the dependence of the extent of cleavage (during 5 min) ($\alpha = [\Delta P]/S_0$) on the substrate concentration ($S_0 = [RNA]$) (Fig. 6, Table 2).

The extent of the cleavage in this case is decreased with increasing substrate concentration in accordance with a modified form, eqn. (6), of the Michaelis equation (1):

$$v_0 = \frac{V_{max} S_0}{K_m + S_0} \qquad (1)$$

where:

$$v_0 = \frac{\Delta P}{\Delta t} \qquad (4)$$

and we have for ΔP:

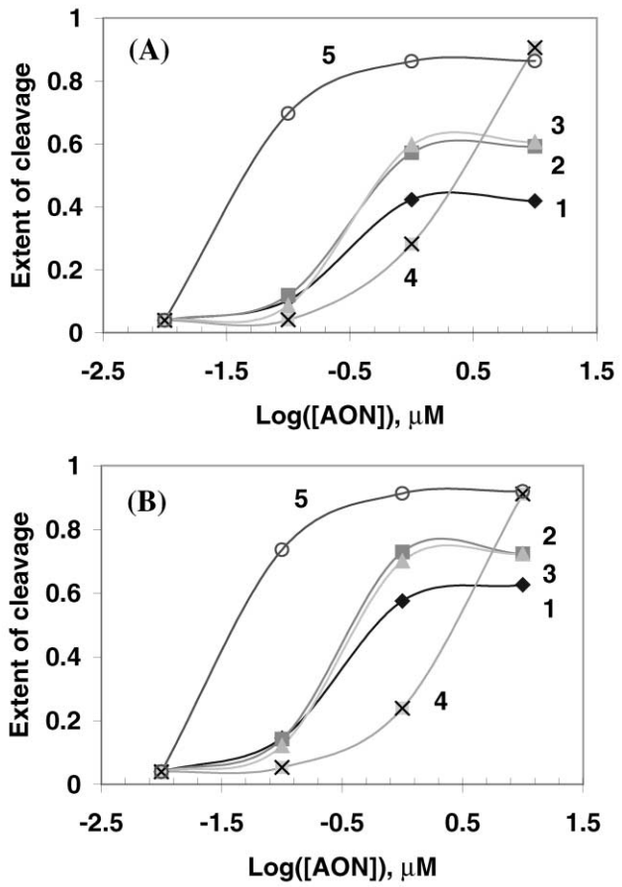

Fig. 3 Extent of hydrolysis of the 17mer target RNA (0.01 μM) in the AON–RNA hybrid duplexes by RNase H as a function of the logarithm of AON concentration (the concentrations of AONs range from 0.01 μM, 0.1 μM, 1 μM and 10 μM. Curves 1–5 in (**A**) and (**B**) correspond to the hybrid duplexes formed by native 9mer AON (**1**), Chol-AON (**2**), Chol(Ac)$_3$-AON (**3**), Cholest-AON (**4**) and Dppz-AON (**5**) respectively. *Conditions of the cleavage reactions:* AON concentration at 0.01–10 μM with constant RNA (**6**) concentration at 0.01 μM in buffer, containing 60 mM Tris-HCl (pH 7.5), 60 mM KCl, 10 mM $MgCl_2$ and 1 mM DTT at 21 °C, 0.5 units in (**A**) and one unit in (**B**) of RNase H. Total reaction volume is 30 μl.

$$\Delta P = v_0 \Delta t = \frac{V_{max} S_0}{K_m + S_0} \Delta t \quad (5)$$

and using eqns. (1), (4) and (5) we can find the dependence of the extent of cleavage ($\alpha = \Delta P/S_0$) on the substrate concentration S_0:

$$\alpha = \frac{\Delta P}{S_0} = \frac{V_{max} S_0}{(K_m + S_0) S_0} \Delta t = \frac{V_{max} \Delta t}{(K_m + S_0)} \quad (6)$$

Eqn. (6) shows that at low substrate concentration (S_0) (when $S_0 \ll K_m$), the extent of the cleavage is not dependent upon the substrate concentration because, when $S_0 \ll K_m$, eqn. (6) can be written as eqn. (7):

$$\alpha = \frac{V_{max} \Delta t}{(K_m + S_0)} = \frac{V_{max}}{K_m} \Delta t \quad (7)$$

In this case, the extent of the cleavage is dependent only on retention of V_{max}/K_m and on reaction time Δt which is always the same (Δt was equal to 5 min in our experiments).

Eqn. (7) explains our experimental data, where Dppz-AON has maximal cleavage compared with all other AONs, in a situation when the substrate concentration is less than the K_m value (Table 3, see the area around S_0 = 0.1 μM in Fig. 6) because the Dppz-AON–RNA substrate has a maximal value of V_{max}/K_m (Fig. 7C).

But, when substrate concentration is increasing, the extent of the cleavage should decrease and become close to zero according to eqn. (6), and this dependence has a hyperbolic shape (see area around S_0 more than 0.1 μM in Fig. 6A).

Thus, our conjugated AONs have better cleaving characteristics both in terms of initial velocity and the extent of the cleavage than the native 9mer AON under low RNA concentration conditions (0.1 micromoles per litre), as under physiological conditions.

The turnover (N_t) of RNase H can be calculated by using eqn. (8):

$$N_t = \frac{P_t}{E_0} \quad (8)$$

where N_t indicates the number of RNA molecules (P_t) that the enzyme cleaves during the time, t. The values for k_{cat} and K_m allow us to define the N_t at a substrate concentration, S_0, according to eqn. (9), which is derived from eqns. (4), (5) and (8):

$$N_t = \frac{\Delta P}{E_0} = \frac{V_{max} S_0}{(K_m + S_0) E_0} \Delta t = \frac{k_{cat} E_0 S_0}{(K_m + S_0) E_0} \Delta t = \frac{S_0}{K_m + S_0} k_{cat} \Delta t = F_e N_{max} \quad (9)$$

where F_e is the extent of saturation of enzyme, E, as shown in eqn. (10), by the substrate, S, which is equal to zero when $[S_0] = 0$, and equal to 1 when $[S_0] \gg K_m$ or $[S_0] \longrightarrow \infty$;

$$F_e = \frac{[ES]}{E_0} = \frac{S_0}{K_m + S_0} \quad (10)$$

ES is the enzyme–substrate complex, and N_{max} is a maximal turn over of enzyme, when the extent of saturation of the enzyme by substrate is maximal, otherwise $F_e = 1$:

$$N_{max} = k_{cat} \Delta t \quad (11)$$

Eqn. (9) means that the turnover of the enzyme is dependent on factors such as the time of reaction, the k_{cat} and F_e [eqn. (10)], which is dependent on both K_m and S_0. It means that at different substrate concentrations S_0, turnover of enzyme, N_t, will be different. We have therefore calculated the values for N_t for each AONs at different substrate concentration during 5 min of reaction (Table 4).

These data show that the turnover of RNase H for Dppz-AON–RNA (N_t = 17.4) at low RNA concentration ($[S_0]$ = 0.123 μM) is more compared with the native 9mer AON. This is because Dppz-AON–RNA substrate under these conditions saturates the RNase H more (F_e = 0.41 or 41%) compared to the native 9mer AON (N_t = 4.6, F_e = 0.006 or 0.6%). But, at 2 μM substrate concentration, RNase H has nearly the same turnover, N_t (Table 4) because at these conditions values of F_e increase for all AONs.

It should be added that all compared data for v_0, α and N_t were obtained using large concentration of AONs (10 μM) (Fig. 4, 5). Under these conditions, whether Dppz-AON can work better or worse compared to the native 9mer AON, depends entirely only upon the substrate (*i.e.* heteroduplex)

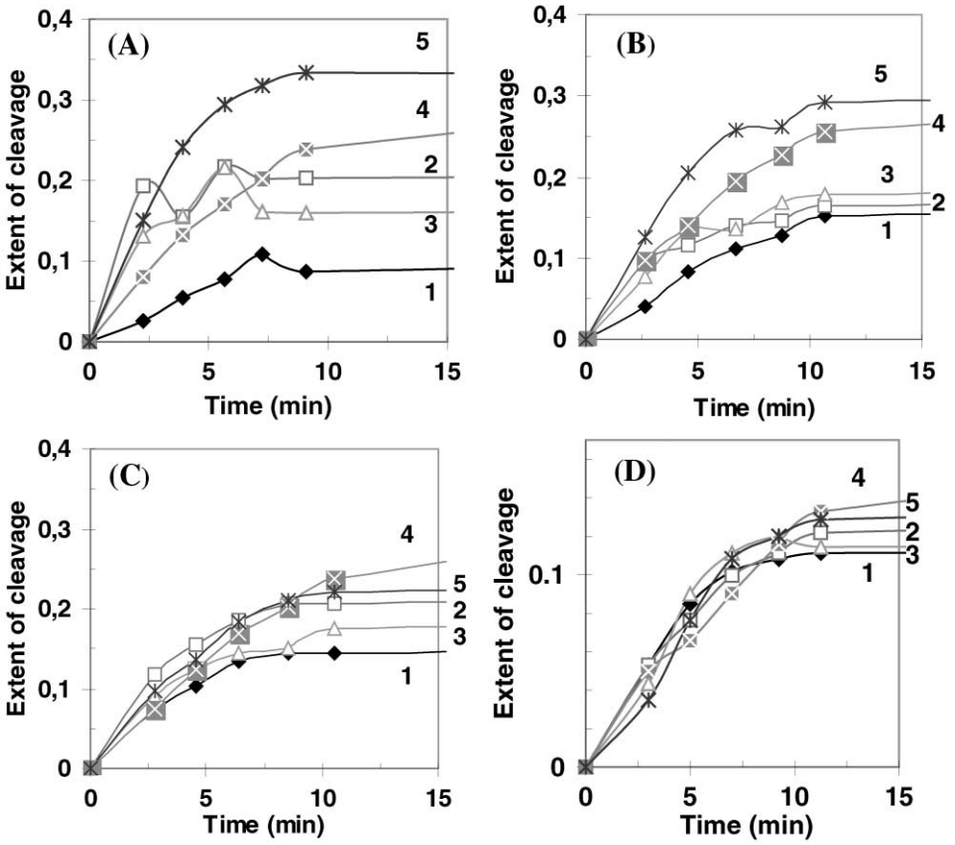

Fig. 4 Extent of hydrolysis of the target RNA (**6**) in the AON–RNA hybrids by RNase H as a function of the reaction time. Curves 1–5 in (**A**) to (**D**) correspond to the hybrid duplexes formed by native 9mer AON (**1**), Chol-AON (**2**), Chol(Ac)$_3$-AON (**3**), Cholest-AON (**4**) and Dppz-AON (**5**) respectively. *Conditions of the cleavage reactions*: AON concentration (10 μM) and RNA (**6**) were varied at 0.123 μM in (**A**), 0.523 μM in (**B**), 1.02 μM in (**C**), and 2.02 μM in (**D**)) in buffer, containing 60 mM Tris-HCl (pH 7.5), 60 mM KCl, 10 mM $MgCl_2$ and 1 mM DTT at 21 °C, 0.5 units of RNase H. Total reaction volume is 30 μl.

concentration. When AON concentration is however low, [AON] = 0.1 μM (Fig. 2A and Fig. 3), all kinetic parameters v_0, a and N_t additionally depend upon the extent of saturation RNA by AON, F_{RNA} [eqn. (12)], which is equal to *ca.* 60% for Dppz-AON and less then 10% for all other AONs (Fig. 3).

The extent of saturation of RNA by AON, F_{RNA}, can be written according to eqn. (12):

$$F_{RNA} = \frac{[DR]}{R_0} = \frac{D_0}{K_D + D_0} \quad (12)$$

where DR is an AON–RNA hybrid duplex, D_0 is initial AON concentration, R_0 is initial RNA concentration and K_D is the equilibrium constant of dissociation of the hybrid AON–RNA.

In conditions when RNA is not saturated by AON and $S_0 \ll K_m$, initial velocity, v_0, or extent of cleavage, a, of reaction, can be rewritten as eqn. (13) or (14) by combining eqns. (2), (6), (12):

$$v_0 = \frac{V_{max}}{K_m} S_0 = \frac{V_{max}}{K_m}[DR] = \frac{V_{max}}{K_m} F_{RNA} R_0 \quad (13)$$

$$\alpha = \frac{\Delta P}{R_0} = \frac{V_{max}[DR]}{(K_m + [DR])R_0}\Delta t = \frac{V_{max}}{K_m}\frac{[DR]}{R_0}\Delta t = \frac{V_{max}}{K_m} F_{RNA}\Delta t \quad (14)$$

According to eqn. (13) the initial velocity of reaction at constant RNA concentration depends upon two parameters: V_{max}/K_m ratio and the thermostability of the AON–RNA duplex, which is maximal for Dppz-AON–RNA substrate compared with other AON–RNA substrates.

The same conclusion can be drawn in the case of the extent of cleavage in Fig. 3. According to eqn. (14) the extent of cleavage during the same time period of reaction depends upon two parameters: V_{max}/K_m ratio as well as on the thermostability of the AON–RNA duplex, and does not depend upon the RNA concentration. Both of these characteristics, value of V_{max}/K_m and F_{RNA}, are much better for Dppz-AON compared with native 9mer AON. This explains why we have different saturation plateaux for different AONs in the AON concentration dependent plots, as shown in Fig. 3. Thus, a maximal extent of RNA cleavage is obtained for Dppz-AON, compared to 9mer AON or other AONs (Fig. 2A and Fig. 3) at 0.1 μM concentration of AON, which is an important characteristic fulfilled by Dppz-AON in order to be a potentially important antisense substance.

The relative retention times of a mixture of AONs **1**–**5** on a reversed-phase C18 column (Fig. 8) showing the relative hydrophobicity of different 3′-tethered AONs, compared to the native gives an insight, in a model system, into how easily these AONs may penetrate inside the cell. Since cholesterol-tethered AON **4** is retained most in the reversed-phase column, it can be assumed that it might be able to penetrate through the cellular membrane most easily. Since we do not find any correlation between the hydrophobicity of Chol-, Chol(Ac)$_3$- and Cholest-AONs (Fig. 8C) and their kinetic parameters (K_m, V_{max} and k_{cat}) (Fig. 7, Table 3), it is likely that the recognition and kinetic degradation of the RNA in AON–RNA duplex by RNase H is not dictated by the hydrophobic properties of the 3′-tethered moiety in the AONs.

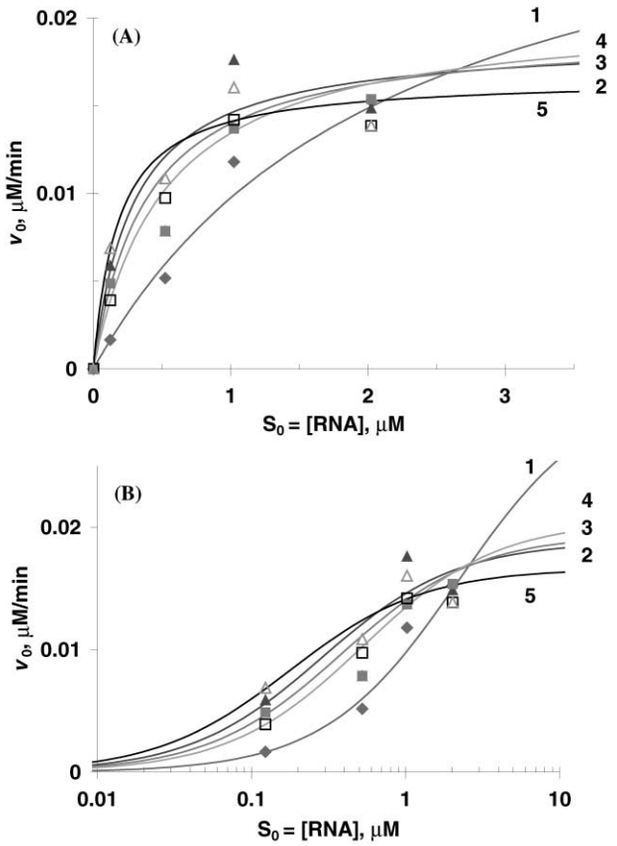

Fig. 5 Initial velocity of the hydrolysis of the 17mer target RNA (**6**) in the AON–RNA hybrids by RNase H as a function of the RNA concentration (the concentrations of RNA range from 1.23×10^{-7} to 2.2×10^{-6} M). Curves 1, 2, 3, 4 and 5 correspond to the hybrid duplexes formed by native 9mer AON (**1**), Chol-AON (**2**), $Chol(Ac)_3$-AON (**3**), Cholest-AON (**4**) and Dppz-AON (**5**) respectively. *Conditions of cleavage reaction*: AON (**1**, **2**, **3**, **4** or **5**) (10 μM) and RNA (**6**) in buffer, containing 60 mM Tris-HCl (pH 7.5), 60 mM KCl, 10 mM $MgCl_2$ and 1 mM $MgCl_2$ and 1 mM DTT at 21 °C, 0.5 U of RNase H. Total reaction volume is 30 μl: (**A**) normal hyperbolic plots, and (**B**) logarithmic scale of S_0 concentration (sigmoidal plots).

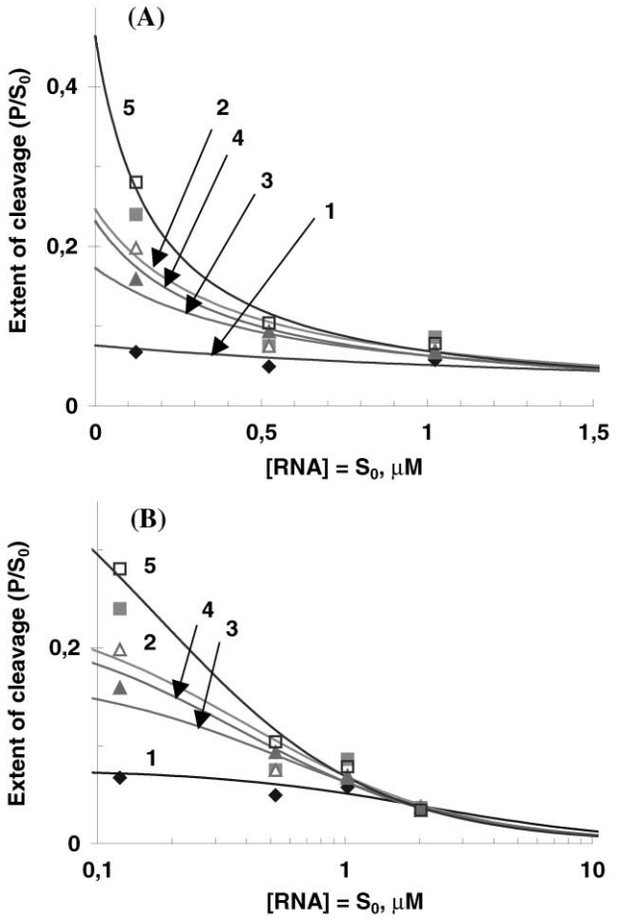

Fig. 6 Extent of cleavage (P/S_0, where P is the amount of cleavage product formed and S_0 is the initial concentration of the substrate (*i.e.* hybrid duplex) of the 17mer target RNA (**6**) in the AON–RNA hybrids by RNase H as a function of the RNA concentration (the concentrations of RNA range from 1.23×10^{-7} to 2.2×10^{-6} M): (**A**) normal hyperbolic plots, and (**B**) on the logarithmic scale, giving sigmoidal plots, of S_0 concentration. Curves 1, 2, 3, 4 and 5 correspond to the hybrid duplexes formed by native 9mer AON (**1**), Chol-AON (**2**), $Chol(Ac)_3$-AON (**3**), Cholest-AON (**4**) and Dppz-AON (**5**) respectively. They show that under saturation conditions of RNA by AON, the extent of the cleavage reaction of the complementary RNA by RNase H slows down as the concentration of RNA goes up. *Conditions of cleavage reaction*: AON (**1**, **2**, **3**, **4** or **5**) (10 μM) and RNA (**6**) in buffer, containing 60 mM Tris-HCl (pH 7.5), 60 mM KCl, 10 mM $MgCl_2$ and 1 mM DTT at 21 °C, 0.5 U of RNase H. Total reaction volume is 30 μl.

Materials and methods

Materials

T4 polynucleotide kinase (30 units per μL) and *E. coli* RNase H (5 units per μL, specific activity 420000 units mg^{-1}, molecular weight 21000 g mol^{-1}) and [γ-^{32}P]ATP were purchased from Amersham Pharmacia Biotech (Sweden), phosphodiesterase I from *Crotalus adamanteus* venom was from SIGMA. Oligonucleotide (**1**)[22a] and RNA (**6**) were synthesized using an Applied Biosystems 392 automated DNA/RNA synthesizer. Syntheses of the 3′-conjugated AONs (**2**–**5**) were carried out by post synthetic methods starting from the same 3′-phosphate tethered 9mer oligonucleotide (**1**), which was conjugated with amino derivatives of the corresponding cholic acid,[20a] 3,7,12-tri-*O*-acetylcholic acid,[20b] cholesterol[20f] or dipyridophenazine[21] as previously described[22] (Scheme 2). All AONs **1**–**5** were characterized by NMR, UV, electrophoresis and enzymatic digestions and compared with the physicochemical properties reported in the literature.[20a,b,f,21,22] The column chromatographic separations were performed using Merck G 60 silica gel. A Bischoff HPLC equipment with Pump Model 2250, Manometric Module Lambda 1010 connected to a DataApex CSW computer program for gradient control were used for analytical and semi-preparative RP-HPLC separations on Kromasil 100 C18 column (5 μm, 250 × 8 mm).

UV melting experiments

Determination of the T_m values of the AON–RNA hybrid duplexes was carried out in the same buffer as for RNase H degradation: 20 mM Tris-HCl (pH 8), 100 mM KCl and 10 mM $MgCl_2$. Absorbance was monitored at 260 nm in the temperature range from 3 °C to 70 °C using Lambda 40 UV spectrophotometer equipped with Peltier temperature programmer with the heating rate of 1 °C per minute. Prior to the measurements samples (1 : 1 mixture of 1 μl AON and 1 μl RNA) were preannealed by heating to 80 °C for 5 min followed by slow cooling to 3 °C and 30 min equilibration at this temperature.

^{32}P Labeling of oligonucleotides

The oligoribonucleotide and oligodeoxyribonucleotides were 5′-end labeled with ^{32}P using T4 polynucleotide kinase, [γ-^{32}P]-ATP and standard procedure. Labeled RNAs were purified by 20% 7 M urea denaturing polyacrylamide denaturing gel

Table 4 Turnovers (N_t and N_{max}) and extent of saturation of enzyme by AON–RNA substrates, F_e, for RNase H cleavage reactions at different substrate concentrations, S_0

Substrate	[RNA] = S_0/μM	$F_e = ES/S_0 = S_0/(K_m + S_0)$	$N_{max} = V_{max}t/E_0 = k_{cat}t$	$N_t = F_eN_{max}$	$N_{relative} = N_t$(AON)/N_t(9mer)
9mer-AON(**1**)–RNA(**6**)	0.123	0.055	83.1	4.6	1
Chol-AON(**2**)–RNA(**6**)	0.123	0.239	50.3	12.0	2.6
Chol$(Ac)_3$-AON(**3**)–RNA(**6**)	0.123	0.176	51.8	9.1	2.0
Cholest-AON(**4**)–RNA(**6**)	0.123	0.246	45.3	11.2	2.4
Dppz-AON(**5**)–RNA(**6**)	0.123	0.413	42.2	17.4	3.8
9mer-AON(**1**)–RNA(**6**)	0.523	0.199	83.1	16.6	1
Chol-AON(**2**)–RNA(**6**)	0.523	0.572	50.3	28.7	1.7
Chol$(Ac)_3$-AON(**3**)–RNA(**6**)	0.523	0.476	51.8	24.7	1.5
Cholest-AON(**4**)–RNA(**6**)	0.523	0.582	45.3	26.4	1.6
Dppz-AON(**5**)–RNA(**6**)	0.523	0.749	42.2	31.6	1.9
9mer-AON(**1**)–RNA(**6**)	1.023	0.328	83.1	27.2	1
Chol-AON(**2**)–RNA(**6**)	1.023	0.723	50.3	36.4	1.3
Chol$(Ac)_3$-AON(**3**)–RNA(**6**)	1.023	0.640	51,8	33.2	1.2
Cholest-AON(**4**)–RNA(**6**)	1.023	0.731	45.3	33.1	1.2
Dppz-AON(**5**)–RNA(**6**)	1.023	0.854	42,2	36.0	1.3
9mer-AON(**1**)–RNA(**6**)	2.023	0.491	83.1	40.8	1
Chol-AON(**2**)–RNA(**6**)	2.023	0.838	50.3	42.1	1.0
Chol$(Ac)_3$-AON(**3**)–RNA(**6**)	2.023	0.778	51.8	40.4	0.99
Cholest-AON(**4**)–RNA(**6**)	2.023	0.843	45.3	38.2	0.94
Dppz-AON(**5**)–RNA(**6**)	2.023	0.920	42.2	38.8	0.95
9mer-AON(**1**)–RNA(**6**)	4	0.656	83.1	54.5	1
Chol-AON(**2**)–RNA(**6**)	4	0.911	50.3	45.8	0.84
Chol$(Ac)_3$-AON(**3**)–RNA(**6**)	4	0.874	51.8	45.3	0.83
Cholest-AON(**4**)–RNA(**6**)	4	0.914	45.3	41.4	0.76
Dppz-AON(**5**)–RNA(**6**)	4	0.958	42.2	40.4	0.74

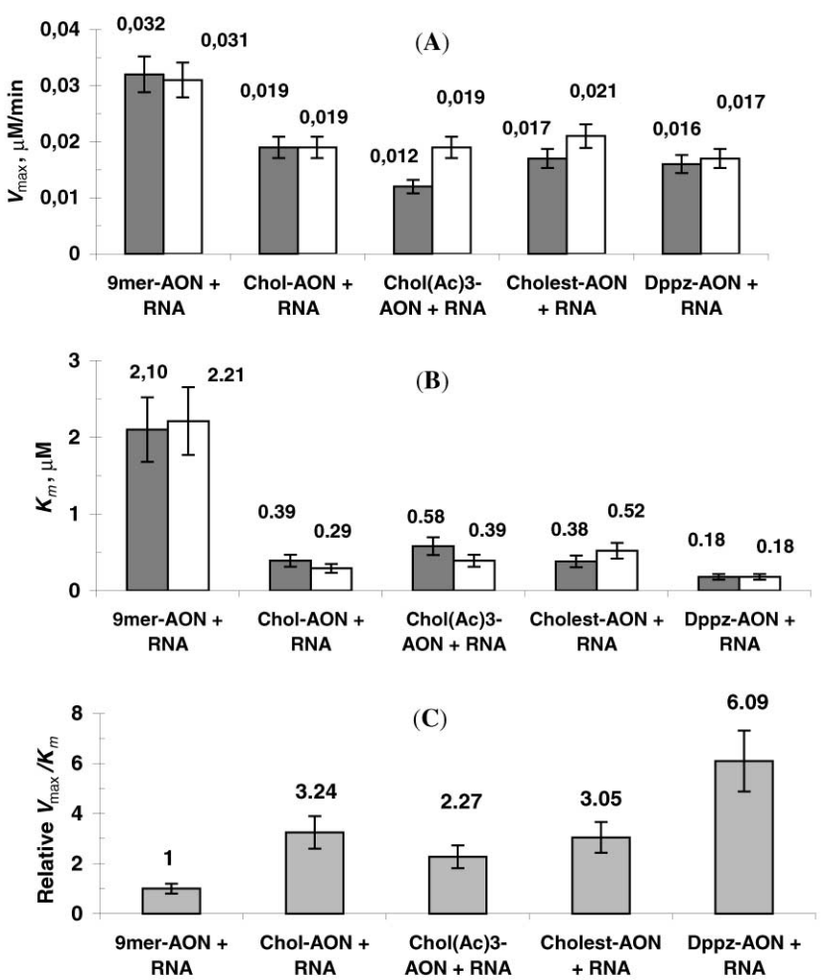

Fig. 7 (**A**) and (**B**) V_{max} and K_m values for the RNase H promoted hydrolysis of AON (**1**–**5**)–RNA (**6**) substrates were determined by a plot of $1/v_o$ versus $1/[S]_0$ (open bars) and Michaelis equation (filled bars). (**C**) Comparison of the V_{max}/K_m values. The relative V_{max}/K_m value for each tethered AON (**2**–**5**)–RNA duplex hybrid duplex was obtained by dividing the V_{max}/K_m value for each tethered AON (**2**–**5**)–RNA duplex by the corresponding value for AON (**1**)–RNA duplex.

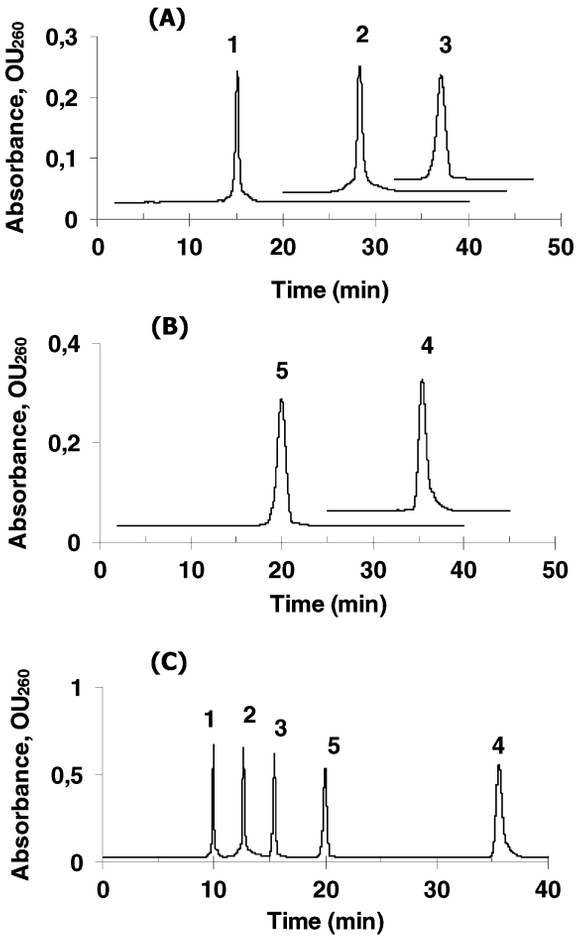

Fig. 8 Analytical C18 reversed-phase HPLC of AONs (**1**–**5**). (**A**): AONs **1**–**3** with t_R = 15.1 min, 28.3 min, 37.2 min, respectively; (**B**): AONs **4** and **5** with t_R = 35.4 min, 20.0 min, respectively; (**C**): Coinjection of an artificial mixture of all AONs **1**–**5**, showing their relative hydrophobic retention times in the C18 reversed-phase column: t_R = 9.9 min, 12.6 min, 15.4 min, 35.6 min and 19.9 min, respectively. *Conditions of chromatography*. (**A**) buffer A: 0.05 M $LiClO_4$, buffer B: 50% CH_3CN in 0.05 M $LiClO_4$, 0% ⟶ 100% B, linear gradient during 50 min, rate of elution 1.5 ml min^{-1}; (**B**) and (**C**) buffer A: 0.05 M $LiClO_4$, buffer B: 80% CH_3CN in 0.05 M $LiClO_4$, 0% ⟶ 100% B, linear gradient during 40 min, rate of elution 1.5 ml min^{-1}.

electrophoresis (PAGE) and specific activities were measured using a Beckman LS 3801 counter.

Snake venom PDE ladder

5′-[^{32}P]-labeled RNA (1.3 μM, specific activity 500000 cpm) was incubated with 100 ng of the phosphodiesterase I in buffer, containing 50 mM Tris-HCl (pH 8), 5 mM $MgCl_2$ at 21 °C. Total reaction volume was 50 μl. After 2, 10, 15, 30, 40 and 60 minutes aliquots (correspondingly 5, 6, 9, 9, 9 and 10 μl) were mixed with stop solution (correspondingly 10, 12, 18, 18, 18 and 20 μl), containing 0.05 M disodium salt of ethylenediaminetetraacetic acid (EDTA), 0.05% (w/v) bromophenol blue and 0.05% (w/v) xylene cyanol in 95% formamide. All aliquots were combined and subjected to 20% 7 M urea polyacrylamide denaturing gel electrophoresis and visualized by autoradiography.

Kinetics

AON concentration dependent experiments. AONs (0.1 μM, 1 μM, or 1 μM), with ^{32}P-labeled RNA (0.01 μM, specific activity 50 000 cpm) were incubated with 0.5 or 1 units of RNase H in buffer, containing 20 mM Tris-HCl (pH 8), 100 mM KCl, 10 mM $MgCl_2$ and 1 mM DTT at 21 °C. Total reaction volume was 30 μl. Prior to the addition of the enzyme reaction components were preannealed in the reaction buffer by heating at 80 °C for 5 min followed by 1.5 h equilibration at 21 °C. After 3–120 minutes aliquots (5 μl) were mixed with stop solution (5 μl), containing 0.05 M disodium salt of ethylenediaminetetraacetic acid (EDTA), 0.05% (w/v) bromophenol blue and 0.05% (w/v) xylene cyanol in 95% formamide. This samples were subjected to 20% 7 M urea polyacrylamide denaturing gel electrophoresis and visualized by autoradiography. Quantitation of cleavage products was performed using a Molecular Dynamics PhosphorImager.

RNA concentration dependent experiments. ^{32}P-Labeled RNA (0.123 μM, 0.523 μM, 1.02 μM or 2.02 μM, specific activity 50 000 cpm) with AONs (10 μM) were incubated with 0.5 units of RNase H in buffer, containing 60 mM Tris-HCl (pH 7.5), 60 mM KCl, 10 mM $MgCl_2$ and 1 mM DTT at 21 °C. Total reaction volume was 30 μl. Prior to the addition of the enzyme reaction components were preannealed in the reaction buffer by heating at 80 °C for 5 min followed by 1.5 h equilibration at 21 °C. After 3–10 minutes aliquots (5 μl) were mixed with stop solution (5 μl) and subjected to 20% 7 M urea denaturing gel electrophoresis. The kinetic parameters K_m and V_{max} were obtained by two methods: from the $1/v_0$ *versus* $1/[S_0]$ plots, where $[S_0]$ = [RNA], or directly from v_0 *versus* $[S_0]$ plots. Values of K_m and V_{max} at the last method were determined directly from v_0 *versus* $[S_0]$ plots by using of correlation SigmaPlot Program, where correlation equation was: $y = ax/(b + x)$.

Acknowledgements

Authors thank the Swedish Natural Science Research Council and the Science Research Council for Engineering Sciences (TFR) for generous financial support.

References

1 M. Itaya and K. Kondo, *Nucleic Acids Res.*, 1991, **19**, 4443.
2 M. Itaya, D. McKelvin, S. K. Chatterjie and R. J. Crouch, *Mol. Gen. Genet.*, 1991, **227**, 438.
3 S. Kanaya and M. Itaya, *J. Biol. Chem.*, 1992, **267**, 10184.
4 W. Busen, *J. Biol. Chem.*, 1980, **255**, 9434.
5 Y. W. Rong and P. L. Carl, *Biochemistry*, 1990, **29**, 383.
6 P. S. Eder, R. Y. Walder and J. A. Walder, *Biochimie*, 1993, **75**, 123.
7 (*a*) S. Kanaya and M. Ikehara, 'Subcell Biochemistry', in *Proteins: Structure, Function, and Engineering*, ed. B. B. Biswas and Siddhartha Roy, Plenium Press, New York, 1995, vol. 24, pp. 377–422; (*b*) I. Lebedeva and C. A. Stein, *Annu. Rev. Pharmacol. Toxicol.*, 2001, **41**, 403–419; (*c*) S. T. Crooke, *Antisense Nucleic Acid. Drug. Dev.*, 1998, **8**, 133–134; (*d*) S. T. Crooke, *Biotechnol. Genet. Eng. Rev.*, 1998, **15**, 121–157; (*e*) S. T. Crooke, *Biochim. Biophys. Acta*, 1999, **1489**, 31–44; (*f*) S. Kanaya, 'Enzymatic activity and protein stability of *E. coli* ribonuclease HI', in *Ribonucleases H*, R. J. Crouch, ed. INSERM, Paris, 1998, Ch. 1, pp. 1–37; (*g*) J. J. Toulme, P. Frank, R. J. Crouch, 'Human ribonuclease H.' in *Ribonucleases H*, ed. R. J. Crouch, INSERM, Paris, 1998, Ch. 7, pp. 147–162; (*h*) J. T. Miller, J. W. Rausch and S. F. Le Grice, *Methods Mol. Biol.*, 2001, **160**, 335–354; (*i*) R. V. Giles and D. M. Tidd, *Methods Mol. Biol.*, 2001, **160**, 157–82; (*j*) E. Zamaratski, P. I. Pradeepkumar and J. Chattopadhyaya, *J. Biochem. Biophys. Methods*, 2001, **48**, 189–208.
8 S. Iwai, M. Wakasa, E. Ohtsuka, S. Kanaya, A. Kidera and H. Nakamura, *J. Mol. Biol.*, 1996, **263**, 699.
9 (*a*) W. F. Lima and S. T. Crooke, *Biochemistry*, 1997, **36**, 390; (*b*) K.-H. Altman, R. Kesselring, E. Francotte and G. Rihs, *Tetrahedron Lett.*, 1994, **35**, 2331; (*c*) M. A. Siddiqui, H. Ford, C. George and V. E. Marquez, *Nucleosides Nucleotides*, 1996, **15**, 235; (*d*) V. E. Marquez, M. A. Siddiqui, A. Ezzitouni, P. Russ, J. Wang, W. R. Wanger and D. M. Matteucci, *J. Med. Chem.*, 1996, **39**, 3739; (*e*) S. Obika, D. Nanbu, Y. Hari, K. Morio, Y. In, T. Ishida and T. Imanishi, *Tetrahedron Lett.*, 1997, **38**, 8735; (*f*) A. A. Koshkin, S. K. Singh, P. Nielson, V. K. Rajwanshi, R. Kumar, M. Meldgaard and J. Wengel, *Tetrahedron*, 1998, **54**, 3607; (*g*) G. Wang, J.-L. Giradet and E. Gunic, *Tetrahedron*, 1999, **55**, 7707; (*h*) J. Wengel, *Acc. Chem. Res.*, 1999, **32**, 301; (*i*) G. Wang,

E. Gunic and J.-L. Giradet, *Bioorg. Med. Chem. Lett.*, 1999, **9**, 1147; (*j*) S. Obika, D. Nanbu, Y. Hari, K. Morio, J. Andoh, K. Morio, T. Doi and T. Imanishi, *Tetrahedron Lett.*, 1998, **39**, 5401; (*k*) M. Sekine, O. Kurasawa, K. Shohda, K. Seio and T. Wada, *J. Org. Chem.*, 2000, **65**, 3571; (*l*) K.-H. Altman, R. Imwinkelried, R. Kesselring and G. Rihs, *Tetrahedron Lett.*, 1994, **35**, 7625; (*m*) S. Obika, K. Morio, Y. Hari and T. Imanishi, *Chem. Commun.*, 1999, 2423; (*n*) S. Obika, K. Morio, Y. Hari and T. Imanishi, *Bioorg. Med. Chem. Lett.*, 1999, **9**, 515; (*o*) R. Steffens and C. Leumann, *Helv. Chim. Acta*, 1997, **80**, 2426; (*p*) R. Buff and J. Hunziker, *Bioorg. Med. Chem.*, 1998, 521.

10 M. J. Damha, C. J. Wilds, A. Noronha, I. Brukner, G. Borkow, D. Arion and M. A. Parniak, *J. Am. Chem. Soc.*, 1998, **120**, 12976.

11 E. Kanaya and S. Kanaya, *Eur. J. Biochem.*, 1995, **231**, 557.

12 L. Kvaerno and J. Wengel, *Chem. Commun.*, 2001, 1419–1424.

13 R. J. Crouch and M.-L. Diksen, in *Nucleases*, ed. S. M. Linn and R. J. Robert, Cold Spring Harbor Laboratory, Cold Spring Harbor, NY, 1982, pp. 211–241.

14 P. Acharya, A. Trifonova, C. Thibaudeau, A. Foldesi and J. Chattopadhyaya, *Angew. Chem., Int. Ed.*, 1999, **38**, 3645.

15 C. Thibaudeau and J. Chattopadhyaya, in *Stereoelectronic Effects in Nucleosides and Nucleotides and their Structural Implications*, Dept of Bioorganic Chemistry, Uppsala University Press, Uppsala, Sweden, 1999.

16 (*a*) P. B. Monia, E. A. Lesnik, C. Gonzalez, W. F. Lima, D. McGee, C. J. Guinosso, A. M. Kawasaki, P. D. Cook and S. M. Frier, *J. Biol. Chem.*, 1993, **268**, 14514; (*b*) P. D. Cook, in *Antisense Research and Applications*, ed. S. T. Crooke and B. Lebleu, CRC Press Inc., Boca Raton, FL, 1993; (*c*) H. Inoue, Y. Hayase, S. Iwai, K. Miura and E. Ohtsuka, *Nucleic Acids Res.*, 1987, **15**, 6131; (*d*) H. Inoue, Y. Hayase, S. Iwai and E. Ohtsuka, *FEBS Lett.*, 1987, **215**, 327; (*e*) T. Kogoma, N. L. Subia and K. Meyenberg, *Mol. Gen. Genet.*, 1985, **200**, 103; (*f*) A. I. Lamond and B. S. Sproat, *FEBS Lett.*, 1993, **325**, 123; (*g*) D. A. Braasch and D. R. Corey, *Chem. Biol.*, 2001, **8**, 1; (*h*) M. Manoharan, *Biochim. Biophys. Acta*, 1999, **1489**, 117; (*i*) K. H. Altmann, D. Fabbro, N. M. Dean, T. Geiger, B. P. Monia, M. Muller and P. Nicklin, *Biochem. Soc. Trans.*, 1996, **24**, 630; (*j*) B. S. Sproat and A. I. Lamond, in *Antisense Research and Applications*, ed. S. T. Crooke and B. Lebleu, CRC Press, Inc., Boca Raton, FL, 1993.

17 (*a*) P. I. Pradeepkumar, E. Zamaratski, A. Földesi and J. Chattopadhyaya, *Tetrahedron Lett.*, 2000, **41**, 8601; (*b*) P. I. Pradeepkumar, E. Zamaratski, A. Földesi and J. Chattopadhyaya, *J. Chem. Soc., Perkin Trans. 2*, 2001, 402; (*c*) P. I. Pradeepkumar and J. Chattopadhyaya, *J. Chem. Soc., Perkin Trans. 2*, 2001, 2074–2083.

18 (*a*) N. Puri, E. Zamaratski, C. Sund and J. Chattopadhyaya, *Tetrahedron*, 1997, **53**, 10409; (*b*) N. Puri and J. Chattopadhyaya, *Nucleosides Nucleotides*, 1999, **18**, 2785; (*c*) E. Zamaratski and J. Chattopadhyaya, *Tetrahedron*, 1998, **54**, 8183; (*d*) E. Zamaratski, D. Ossipov, P. I. Pradeepkumar, N. Amirkhanov and J. Chattopadhyaya, *Tetrahedron*, 2001, **57**, 593; (*e*) N. V. Amirkhanov, E. Zamaratski and J. Chattopadhyaya, *Tetrahedron Lett.*, 2001, **42**, 489.

19 (*a*) T. V. Maltseva, P. Agback, M. N. Repkova, A. G. Venyaminova, E. M. Ivanova, A. Sandstrom and J. Chattopadhyaya, *Nucleic Acids Res.*, 1994, **22**, 559; (*b*) T. V. Maltseva, P. Agback and J. Chattopadhyaya, *Nucleic Acids Res.*, 1993, **21**, 4246; (*c*) T. V. Maltseva and J. Chattopadhyaya, *Tetrahedron*, 1995, **51**, 5501; (*d*) T. V. Maltseva, V. F. Zarytova and J. Chattopadhyaya, *Biochem. Biophys. Methods*, 1995, **30**, 163.

20 (*a*) C. F. Bleczinski and C. Richert, *J. Am. Chem. Soc.*, 1999, **121**, 10889; (*b*) H. Gao and J. R. Dias, *Synth. Commun.*, 1997, **27**, 757; (*c*) W. Kramer and G. Wess, *Eur. J. Clin. Invest.*, 1996, **26**, 715; (*d*) T. J. Lehmann and J. W. Engels, *Bioorg. Med. Chem.*, 2001, **9**, 1827; (*e*) D. Opsenica, G. Pocsfalvi, Z. Juranic, B. Tinant, J. P. Declercq, D. E. Kyle, W. K. Milhous and B. A. Solaja, *J. Med. Chem.*, 2000, **43**, 3274; (*f*) R. L. Letsinger, G. Znang, D. K. Sun, T. Ikeuchi and P. S. Sarin, *Proc. Natl. Acad. Sci. USA*, 1989, **86**, 6553; (*g*) G. Godard, A. S. Boutorin, E. Saison-Behmoaras and C. Helene, *FEBS Lett.*, 1995, **232**, 404.

21 D. Ossipov, E. Zamaratski and J. Chattopadhyaya, *Helv. Chim. Acta*, 1999, **82**, 2186.

22 (*a*) T. Horn and M. S. Urdea, *Tetrahedron Lett.*, 1986, **27**, 4705; (*b*) V. F. Zarytova, T. S. Godovikova, I. V. Kutyavin and L. M. Khalimskaya, 'Reactive oligonucleotide derivatives as affinity reagents and probes in molecular biology', in *Biophosphates and their Analogues—Synthesis, Structure, Metabolism and Activity*, ed. K. S. Bruzik and W. J. Stec, Elsevier, Amsterdam, 1987, p. 149; (*c*) D. V. Pyshnyi, I. A. Pyshnaya, S. G. Lokhov, E. M. Ivanova and V. F. Zarytova, *Russian J. Bioorg. Chem.*, 1995, **21**, 612.

23 (*a*) S. T. Crooke, M. J. Graham, J. E. Zuckerman, D. Brooks, B. S. Conklin, L. L. Cummins, M. J. Greig, C. J. Guinosso, D. Kornbrust, M. Manoharan, H. M. Sasmor, T. Schleich, K. L. Tivel and R. H. Griffey, *J. Pharmacol. Exp. Ther.*, 1996, **277**, 923; (*b*) M. Manoharan, L. K. Johnson, C. F. Bennet, T. A. Vickers, D. J. Ecker, L. M. Cowsert, M. Frier and P. D. Cook, *Bioorg. Med. Chem. Lett.*, 1994, **4**, 1053; (*c*) A. S. Boutorin, L. V. Gus'kova, E. M. Ivanova, N. D. Kobetz, V. F. Zarytova, A. S. Ryte, L. V. Yurchenko and V. V. Vlassov, *FEBS Lett.*, 1989, **254**, 129; (*d*) A. S. Ryte, V. N. Karamyshev, M. V. Nechaeva, Z. V. Gus'kova, E. M. Ivanova, V. F. Zarytova and V. V. Vlassov, *FEBS Lett.*, 1992, **299**, 124.

24 M. Dixon and E. C. Webb, in *Enzymes*, 3rd edn., Longman Group Limited London associated companies, published by Academic Press Inc., New York, 1979, p. 60.

25 A. Fersht, *Enzyme Structure and Mechanism*, 2nd edn., Freeman, New York, 1985.